Pergamon

Biochemical Pharmacology, Vol. 48, No. 2, pp. 391–401, 1994.

0006-2952/94 $7.00 + 0.00

0006-2952(94)E0124-4

SEQUESTRATION OF DOXORUBICIN IN VESICLES IN A MULTIDRUG-RESISTANT CELL LINE (LZ-100)

MARGUERITE A. SOGNIER,* YIN ZHANG, RICHARD L. EBERLE, KEVIN M. SWEET, GUILLERMO A. ALTENBERG† and JAMES A. BELLI

Biology Division, Department of Radiation Therapy, and †Department of Physiology and Biophysics, The University of Texas Medical Branch, Galveston, TX 77555, U.S.A.

(*Received* 6 *July* 1993; *accepted* 14 *February* 1994)

Abstract—A multidrug-resistant Chinese hamster cell line, LZ-8, was subcultured in increasing levels of doxorubicin (DOX) until capable of growth in 100 μg/mL DOX. This new derivative, designated LZ-100, is the most DOX-resistant line in the LZ series, based on a comparison of K_i^{-1} values from cell survival studies. This increased level of drug resistance in LZ-100 cells did *not* result from (i) higher levels of P-glycoprotein (P-gp) in the plasma membrane compared with LZ-8 cells, since this protein constitutes approximately 20% of the total plasma membrane protein in both cell lines, or (ii) more efficient drug pumping by the same amount of P-gp, since efflux of rhodamine 123 and DOX was comparable in the two cell lines. However, an altered drug distribution was observed in LZ-100 cells compared with wild-type V79 cells; in LZ-100 cells DOX was largely excluded from the nucleus and was sequestered in vesicles in the cytoplasm. The number of vesicles per cell seen after DOX exposure corresponded with the level of drug resistance achieved by the LZ cell lines studied. DOX concentration–response experiments revealed that vesicle formation exhibited a biphasic relationship, with an initial rapid increase followed by a plateau where no further increase was observed. Time–course studies in LZ-100 cells revealed that the maximum number of DOX-containing vesicles per cell occurred 3–4 hr following initiation of DOX treatment. Radiation exposure (10 Gy) immediately preceding DOX treatment decreased the number of vesicles formed in LZ-100 cells by more than one-half and altered the subcellular distribution of DOX from an almost exclusively cytoplasmic to a homogeneous nuclear/cytoplasmic distribution. This redistribution was not a result of radiation inhibition of P-gp efflux. The inhibitory effect of radiation on vesicle formation increased with increasing radiation dose up to 10 Gy. Drug-containing vesicles were also observed in LZ-100 cells following exposure to mitoxantrone or daunorubicin (to which LZ-100 cells are also resistant), but fewer vesicles were observed than with DOX. These studies demonstrate that the drug sequestration phenomenon (i) occurs in cells exhibiting widely different levels of drug resistance, (ii) correlates with the level of drug resistance in LZ cell lines, (iii) occurs rapidly following exposure to DOX, mitoxantrone, or daunorubicin, and (iv) can be inhibited by irradiation. Further study of the drug sequestration phenomenon in LZ-100 cells, and its less DOX-resistant precursors LZ-3 and LZ-8, should provide additional insight into this mechanism and its contribution to overall drug resistance.

Key words: P-glycoprotein; drug sequestration; multidrug resistance; doxorubicin; radiation

The multidrug-resistant phenotype can be produced by one or more mechanisms acting singly or in concert [1, 2]. A frequently reported mechanism is P-gp‡-mediated enhanced drug efflux [3–5]. Enhanced drug efflux alone can produce the drug resistance phenotype based on gene transfection studies [6]. However, P-gp-mediated enhanced drug efflux has also been observed in cells exhibiting one or more other, known or putative drug resistance mechanisms, i.e. changes in the activity/levels of detoxification enzymes [7–9], alterations in the quantity/function of topoisomerase II [10], enhanced DNA repair processes [11, 12], altered intracellular drug distribution [13, 14], and the compartmentalization of drug in vesicles away from target sites (for review see Ref. 12). The simultaneous existence of multiple mechanisms in the same cell, designated a "complex" multidrug-resistant phenotype [2], is thought to be a major contributing factor to failure in the treatment of human tumors [1, 2]. Yet, currently, the relative importance of individual mechanisms to overall drug resistance, the temporal sequence for development of these multiple mechanisms, and even some of the mechanisms themselves are not well characterized.

To investigate such questions, our laboratory selected a series of increasingly DOX-resistant cell lines from wild-type V79 Chinese hamster lung cells. These cell lines exhibit the multidrug-resistant phenotype with cross-resistance to vincristine, actinomycin-D, and colcemid as well as P-gp-dependent enhanced drug efflux [15–17]. Contingent on the level of drug resistance attained, the cell lines also exhibit one or more additional resistance mechanisms [18]. To identify other resistance mechanisms, we selected a cell line, designated LZ-100, that is able to grow in 100 μg/mL DOX

* Corresponding author: Dr. Marguerite A. Sognier, U.T.M.B., Department of Radiation Therapy, Mail Route F-56, Galveston, TX 77555. Tel. (409) 772-4228; FAX (409) 772-3387.

‡ Abbreviations: P-gp, P-glycoprotein; FBS, fetal bovine serum; DAUN, daunorubicin; DOX, doxorubicin; MITO, mitoxantrone; MDR, multidrug resistance; and R123, rhodamine 123.

(0.18 mM). These cells were studied to determine the mechanism(s) enabling their growth and survival in the presence of such an elevated drug concentration.

MATERIALS AND METHODS

Cells. V79, 77A, LZ-3, LZ-8, and LZ-24 cells were grown in F10 medium plus 10% FBS with or without DOX (as appropriate) as previously described [19]. The LZ-100 cell line was selected from LZ-24 by growth in F10 medium containing 10% FBS and 50 μg/mL DOX for 7 days, followed by continual growth in 100 μg/mL for more than 1 year. For all LZ cell lines, DOX was removed from the growth medium 24 hr before conducting experiments, unless otherwise specified.

Cell survival. The survival response of the various cell lines was determined by colony-forming ability as described [18]. Exponentially growing cells were exposed to various concentrations of DOX for 1 hr (pretreatment before irradiation) or 3 hr (cell survival) at 37°, rinsed with Puck's Saline A, and subcultured in F10 medium at numbers that would yield 100–200 colonies/treatment. For some experiments, cells were pretreated with DOX, rinsed twice, and exposed to different doses of X-rays using a Picker X-ray machine (50 kVp, 20 mA) before subculturing to determine colony-forming ability, as previously detailed [19]. All experiments were performed a minimum of three times.

Quantitation of P-gp in cell membrane. A Beckman DU-8 Spectrophotometer (Beckman Instruments Inc., Fullerton, CA) was used to quantitate P-gp via gel scanning of proteins separated using polyacrylamide gel electrophoresis and western blotting as described in detail [16]. The amount of protein was quantitated using the Lowry assay. All experiments were performed a minimum of four times.

Visualization of intracellular DOX. The cyto-fluorescence of DOX was analyzed using a Zeiss Axiophot microscope with fluorescence attachment according to the methods described by Chauffert *et al.* [20]. The number of vesicles were quantified by counting the distinctly boundaried, round, red fluorescent bodies present in each cell. No diffuse areas of fluorescence were scored. Since vesicles were present throughout the cytoplasm of the cells, they were enumerated at several different focal planes in an orderly manner (top to bottom of cell) and the numbers summed to determine the total number per cell. Fifty to one hundred cells were evaluated for each experimental treatment, and the mean number of vesicles ± SD was calculated. Each cell was counted/recounted until a consistent number of vesicles was obtained at least twice. Each experiment was performed a minimum of two to three times.

Measurement of drug efflux. The unidirectional efflux of R123 was measured in semiconfluent monolayers of V79, LZ-8, and LZ-100 cells plated the day before on 130–160 μm-thick coverslips. After cells reached steady state (exposure 15 μM R123, 60–90 min, 37°), coverslips were placed in a 200-μL volume chamber on the stage of an inverted microscope (Nikon Diaphot, Tokyo, Japan; oil immersion objective, NA = 1.3, 40x). At time zero, superfusion with a R123-free Ringer's solution was started (20 mL/min), and the decay of intracellular fluorescence was measured for 50–200 cells. The results for LZ-100 cells were normalized to the fluorescence measured for 100 V79 cells loaded to steady-state levels with R123. The excitation and emission wavelengths used were 495 and 535 nm, respectively (535DF25, Omega Optical Inc., Brattleboro, VT) with data acquisition at 1 Hz. Fluorescence measurements were carried out with a Deltascan System (Photon Technology International Inc., South Brunswick, NJ) as previously described [21]. Experiments were performed a minimum of seven times.

Alternatively, the efflux of DOX was measured using fluorescent spectrophotometry with or without pretreatment with 10 Gy radiation as previously described [16]. For these experiments, LZ-100 cells were exposed to 150 μg/mL DOX for 1 hr. Experiments were performed at least twice.

Dot blot analysis. DNA isolation, preparation of dot blots using Hybond N (Amersham) and a Schleicher & Schuell Minifold II manifold, and hybridization with the pCHP1 probe for hamster *pgp* 1 gene were performed according to our previously published protocol [22]. Poly A RNA was isolated using an Invitrogen Fast Track kit according to the manufacturer's specifications. A range of concentrations, from 0 to 5 μg of DNA/RNA, was spotted on the dot blot for analysis to ensure accuracy; however, data for only 3 μg of DNA and 2 μg mRNA are shown in the table. Dot blot experiments were performed many times.

Laser scanning confocal microscopy. V79 and LZ-100 cells exposed to DOX were visualized using a Noran Instruments laser scanning confocal microscope equipped for visualizing DOX. Cells grown on sterile coverslips were exposed to DOX for 2–4 hr (V79 = 10 μg/mL, LZ-100 = 100 μg/mL), placed on the microscope stage in the presence of DOX-containing medium, and then visualized using a 40, 60 or 100X objective. Black and white photographs were taken directly from the images displayed on the video screen.

RESULTS

The level of resistance of the LZ cell lines to DOX was determined by treating exponentially growing cells with various concentrations of DOX for 3 hr (instead of 1-hr treatments as in our previous studies) due to the very high level of resistance exhibited by the LZ-100 cells. The results (Fig. 1) show that as selection in increasingly higher concentrations of DOX progressed, increased cell survival was observed following DOX treatment. This was revealed by comparing the reciprocal of the slope of the initial portion of the survival curve (K_i^{-1}) for the cell lines: LZ-3 = 64 μg/mL, LZ-8 = 786, LZ-24 = 978, LZ-50 = 927 (data not shown in graph) and LZ-100 = 1480.

To determine if the increased drug resistance observed could result from increased drug efflux due to further increases in the levels of P-gp in the

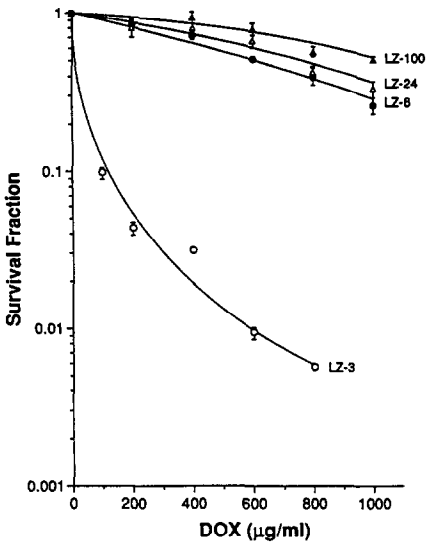

Fig. 1. Survival response of four cell lines in the LZ series to 3-hr DOX treatment. The K_i^{-1} values were 64 μg/mL for LZ-3, 786 for LZ-8, 978 for LZ-24, and 1480 for LZ-100. Values are means ± SD for three independent experiments where all points represent data from triplicate dishes.

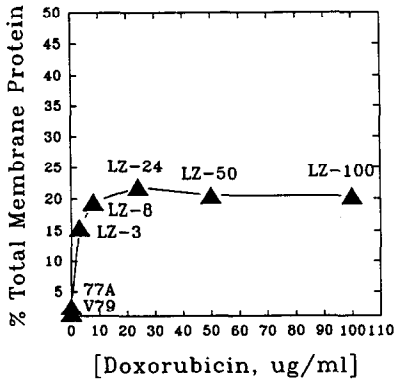

Fig. 2. Levels of P-gp in the LZ cell lines expressed as a percentage of total membrane protein quantitated using gel scanning of Coomassie Blue stained polyacrylamide gels. The horizontal axis represents the concentration of DOX in which LZ cell lines were subcultured continuously.

plasma cell membrane, P-gp levels were determined using gel scanning of Coomassie Blue stained polyacrylamide gels [16]. The results in Fig. 2 show that P-gp levels correspondingly increased with the level of DOX in which the cells were maintained in culture in the early selection stages (77A and LZ-3). P-gp levels reached approximately 20% of the total membrane protein in LZ-8 cells and remained close to this level in LZ-24, LZ-50, and LZ-100 cells. Since P-gp represents the product of the *pgp* 1 gene in hamster lines, measurements of gene amplification

Table 1. Dot blot analysis of isolated DNA and mRNA

Cell lines	DNA (3 μg)	mRNA (2 μg)
V79	4438	2513
LZ-3	116K	97K
LZ-8	131K	186K
LZ-24	159K	211K
LZ-100	103K	161K

Dot blot was hybridized with the pCHP1 probe for hamster *pgp* 1 gene. Numbers represent total counts accumulated in 10 min, assayed using a Packard Instruments Matrix 96 direct beta counter.

and mRNA expression of the *pgp* 1 gene using dot blot hybridization were performed. Analysis of 3 μg of DNA isolated from each cell line revealed a small increase in gene amplification in LZ-24 and a small decrease in LZ-100 (see Table 1, column 2) compared with LZ-8, which contained approximately the same level of P-gp in the plasma cell membrane. Analysis of 2 μg of mRNA from each cell line revealed a somewhat similar pattern (see Table 1, column 3) for mRNA expression of the *pgp* 1 gene. Thus, LZ-100 appears to have a slightly decreased level of gene amplification and less mRNA expression compared with LZ-24 and LZ-8. This suggests the possibility that P-gp in LZ-100 may have increased stability. Overall, these results suggest that differences in levels of P-gp in the plasma membrane are not responsible for the enhanced survival exhibited by LZ-100 cells compared with LZ-8 and LZ-24. Since LZ-8 and LZ-100 cells contain the same amount of P-gp, the differential survival observed may result from: (i) the same number of P-gp molecules eliminating (pumping) drug faster in LZ-100 than in LZ-8 cells; (ii) a larger number of P-gp molecules being active in LZ-100 than in LZ-8 cells; or (iii) the expression of other drug-resistant mechanisms.

To test if the same number of P-gp molecules were pumping more drug in LZ-100 than in LZ-8 cells, the efflux of DOX was determined for LZ-100, LZ-8, and wild-type V79 cells using R123. R123 was used in these studies since DOX-induced multidrug-resistant cells have been shown to be cross-resistant to R123, and increased efflux of this compound has been shown to correlate with increased resistance and *mdr* 1 expression [23, 24]. Upon starting the R123-free superfusion, the rate of decay in cell fluorescence was faster in LZ-8 and LZ-100 cells than in V79 cells, but there was no difference between the former. From the single exponential fit of the data, a rate constant was obtained and a half-time calculated as described [21]. The steady-state R123 fluorescence was calculated from extrapolation to the fluorescence at time zero. The initial 10–15 sec of the fluorescence decay curves denote mixing of extra- and intracellular R123 fluorescence and were not used. Figure 3 illustrates the half-times of the decrease in R123 fluorescence and the steady-state intracellular R123 fluorescence. R123 fluorescence

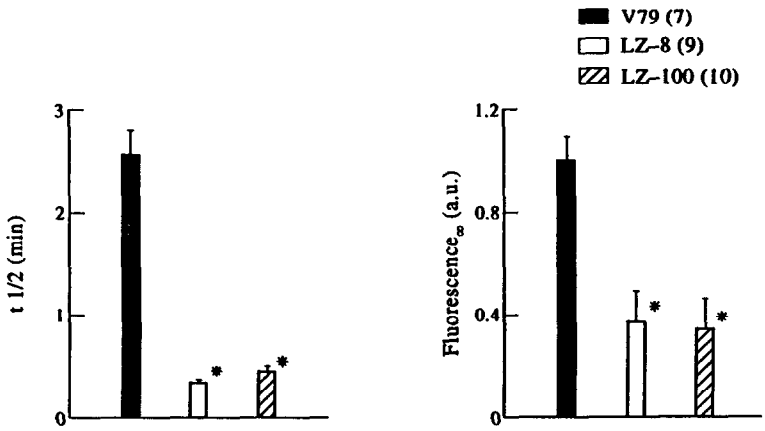

Fig. 3. Steady-state R123 intracellular fluorescence and half-times of unidirectional R123 efflux in V79, LZ-8, and LZ-100 cells. Values are means ± SEM. Asterisks denote a significant difference ($P < 0.05$) from V79 cell values.

was greater in V79 cells than in LZ cells; however, there was no difference between LZ-8 and LZ-100 cells. Additional measurements were made using fluorescent spectrophotometry to quantify the efflux of DOX [16]. The $T_{1/2}$ for LZ-8 and LZ-100 cells treated with 15 and 150 μg/mL for 1 hr, respectively, was 1 min, whereas that of wild-type V79 cells (exposed to 3 μg/mL) was 45 min. Based on both types of measurements, the P-gp present in both the LZ-8 and LZ-100 cell lines pumps drug at the same rate, suggesting that other mechanisms of resistance exist in LZ-100 to account for the enhanced survival after DOX treatment.

In previous studies, we observed that LZ-8 and LZ-24 cells exhibit an altered intracellular drug distribution compared with wild-type V79 cells by analyzing with fluorescent microscopy cells grown on coverslips in the presence of DOX [19]. DOX primarily localized to the cytoplasm, with little or no drug entering the nucleus. In addition, drug-containing vesicles were observed in the cytoplasm. To ascertain if a similar phenomenon was present in LZ-100, the distribution of DOX in cells grown on coverslips in medium containing 100 μg/mL DOX was determined. Figure 4A shows that the nucleus of LZ-100 cells (grown in the presence of their nontoxic maintenance concentration of 100 μg/mL DOX) contained little or no fluorescence compared with the cytoplasm. In addition, these cells exhibited a number of red, fluorescent vesicles that contained DOX based on specific fluorescence wavelength excitation/emission (485 nm excitation: emission 515–585) [20]. Figure 4B is a black and white photograph of identically treated LZ-100 cells obtained using laser scanning confocal microscopy. In this illustration, the nucleus appears dark (indicative of a lack of DOX) while the vesicles appear as bright white (instead of red) circular structures in the cytoplasm. This should be contrasted with wild-type V79 cells in Fig. 4C (also see color, fluorescent microscopy photograph in Ref. 17) where the drug is concentrated in the nucleus (indicated by white color) and few DOX-containing vesicles are observed in the cytoplasm. Analysis of 50–100 cells of the different LZ cell lines grown in their respective maintenance concentrations of DOX (see Table 2) revealed that the mean number of vesicles/cell correlated with the level of resistance exhibited by the cell line, i.e. the most DOX-resistant cell line, LZ-100 (maintained in 100 μg/mL DOX) contained the highest mean number of vesicles/cell, while the least resistant cell line, LZ-3 (grown in 3 μg/mL), exhibited the fewest vesicles per cell with LZ-24 (24 μg/mL DOX) and LZ-8 (8 μg/mL DOX) exhibiting intermediate levels of resistance and a mean number of vesicles/cell. To determine if the difference in mean number of vesicles observed in these cell lines was a function of the concentration of DOX to which the cells were exposed, all LZ cell lines were treated with 100 μg/mL DOX for 2 hr. The results, shown in Fig. 5, reveal that under these conditions, a similar trend was observed, i.e. the greatest number of vesicles was seen in LZ-100 (94 ± 12) and the fewest in LZ-3 (39.1 ± 8). To determine if the LZ cell lines had an infinite or limited capacity to form vesicles, the relationship between drug concentration and number of vesicles observed was determined for each cell line. As shown in Fig. 6, each cell line exhibited a biphasic relationship in which there was an initial rapid increase followed by a plateau where no further increase was observed. To determine the time after exposure when LZ-100 cells would contain the maximum number of vesicles/cell, LZ-100 cells were exposed to 100 μg/mL DOX, and the number of vesicles was determined at various time intervals. In Fig. 7, it can be seen that the maximum number of vesicles was observed at approximately 3 hr. Overall, these results show that: the formation of vesicles represents a rapid response in LZ cell lines (reaching a maximum in about 3–4 hr), LZ-100 has a greater ability to form DOX-containing vesicles than the earlier selection stages of LZ, the number of vesicles formed corresponds with the overall level of DOX

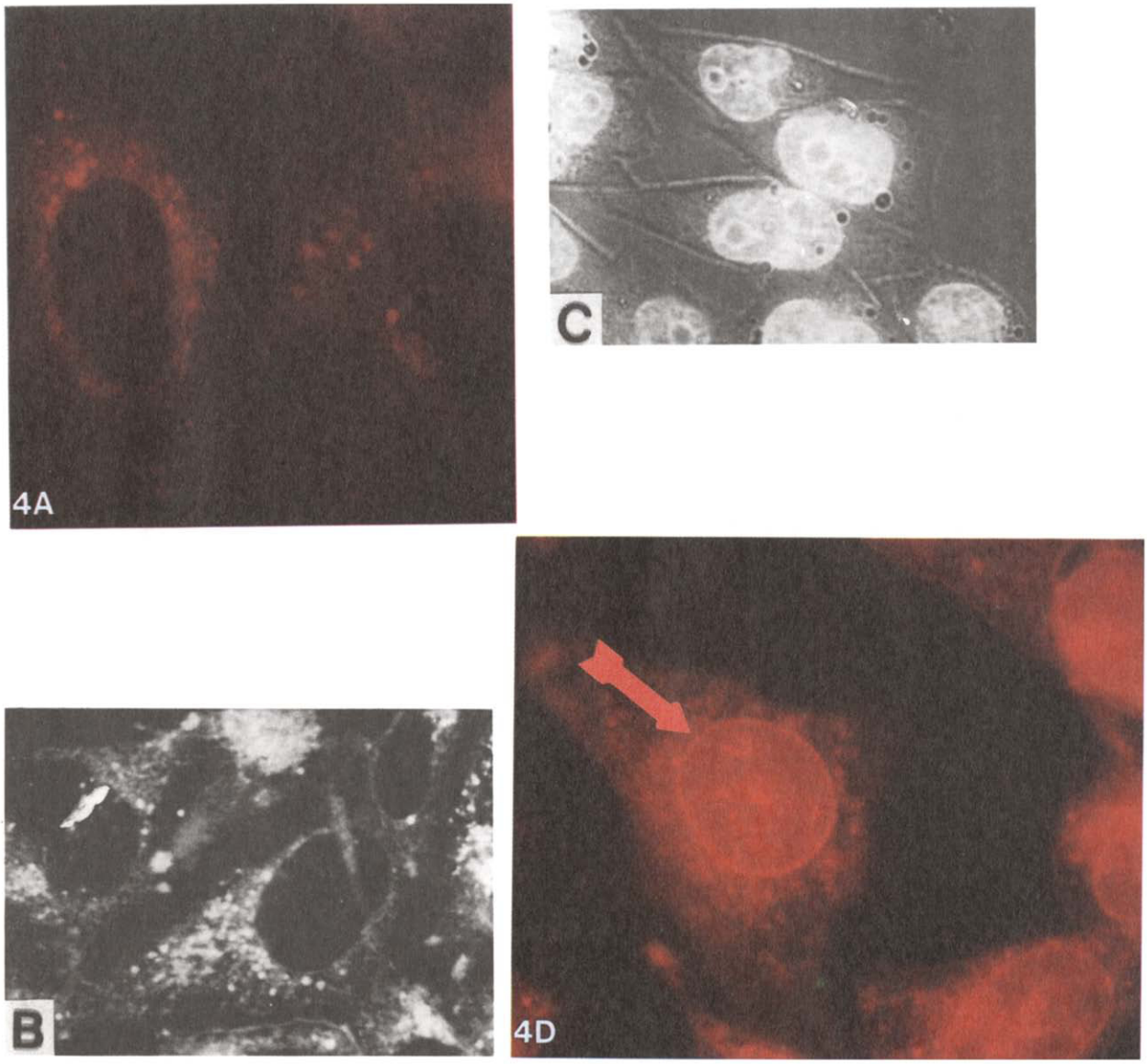

Fig. 4. (A) LZ-100 cell grown in 100 μg/mL DOX and visualized using fluorescent microscopy. Note diminished fluorescence in the nucleus and the presence of red fluorescent vesicles in the cytoplasm. Not all vesicles present are apparent due to their distribution throughout the cytoplasm and location in different focal planes. (B) LZ-100 cells exposed to 100 μg/mL DOX for 2 hr and visualized with confocal microscopy. In the black and white photograph, DOX appears white and is present in vesicles in the cytoplasm of the cells. (C) Wild-type V79 cells exposed to 1 μg/mL DOX for 2 hr and visualized with confocal microscopy. DOX is evident in nucleus of the cells (white color). Both fluorescence and bright field optics were used simultaneously in this exposure to enable plasma membrane of the cells to be visualized. (D) LZ-100 cells pretreated with 10 Gy, then exposed to DOX for 2 hr and visualized with fluorescent microscopy. Note the presence of drug (red color) in the nucleus, indicated by the arrow. Fewer vesicles are seen in the cytoplasm, as in unirradiated, DOX-treated LZ-100 cells.

resistance exhibited by the cell, and either LZ cell lines have a limited ability to form vesicles or an equilibrium is eventually reached between new vesicle formation and extrusion of vesicles from the cell.

Since our observations suggested that the vesicles in LZ cell lines consisted of DOX contained within a membrane, and one effect of radiation exposure is the production of membrane damage [25–27], we tested if radiation exposure could alter (increase or decrease) vesicle formation. Cells treated with 100 μg/mL DOX for 2 hr, both with and without pretreatment with X-rays, were viewed using a fluorescent microscope, and the number of vesicles was quantified. LZ-100 cells treated with 10 Gy at the time of DOX addition (100 μg/mL), incubated

Table 2. Mean number of vesicles per cell in LZ cell lines

Cell line	DOX (μg/mL)	Mean No. of vesicles/cell
LZ-100	100	103 ± 17
LZ-24	24	55 ± 23
LZ-8	8	29 ± 7
LZ-3	3	16 ± 4

Analysis was performed in LZ cell lines grown continuously in their maintenance concentrations of DOX: LZ-3 = 3 μg/mL, LZ-8 = 8 μg/mL, LZ-24 = 24 μg/mL, and LZ-100 = 100 μg/mL.

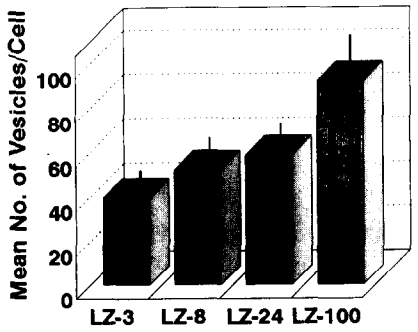

Fig. 5. Effect of exposure to 100 μg/mL DOX for 2 hr on LZ cell lines exhibiting different levels of resistance. The mean number of vesicles per cell was quantified for 50–100 cells, using fluorescent microscopy. Standard deviations are shown.

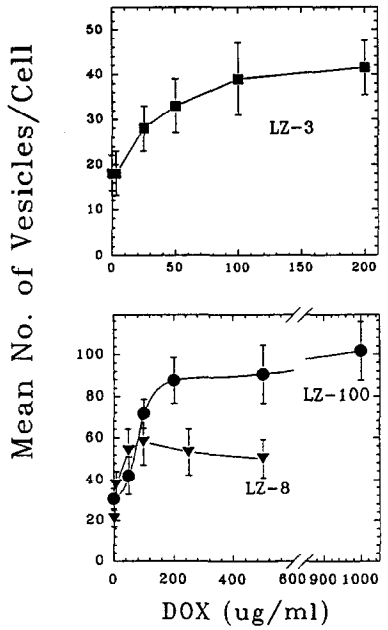

Fig. 6. DOX concentration–response study of LZ cell lines exhibiting different levels of resistance. Cells were exposed to the indicated drug concentrations for 2 hr, and then the mean number of vesicles/cell was quantified. Each point depicts the mean ± SD for ≥50 cells. This graph is representative of the results of one experiment and was consistent with two additional repetitions.

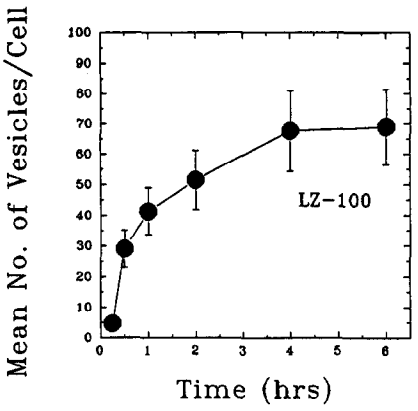

Fig. 7. Time–course study of DOX-induced vesicles in LZ-100 cells. Cells were exposed to 100 μg/mL DOX, and the number of vesicles was determined at the indicated times. Each point depicts the mean ± SD for ≥50 cells. This graph depicts the results of one experiment and was consistent with two additional repetitions.

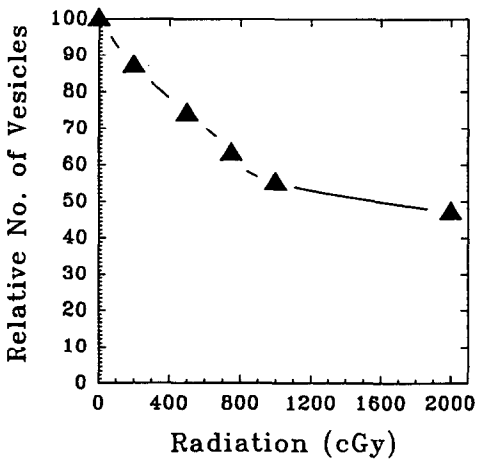

Fig. 8. Radiation dose–response of LZ-100 cells exposed to 0, 2, 5, 7.5, 10, and 20 Gy and then treated with 100 μg/mL DOX. The relative number of vesicles represents the average number of vesicles per cell observed with radiation pretreatment as a fraction of the number of vesicles observed with equivalent DOX treatment without radiation.

in DOX for 2 hr and then evaluated using fluorescent microscopy exhibited less than half the number of vesicles per cell (27 ± 7) than the LZ-100 cells treated with DOX alone (71 ± 13). Control LZ-100 cells that received no drug treatment contained a mean number of 20 ± 6 vesicles per cell, as assayed using phase contrast microscopy (since these vesicles exhibit no fluorescence due to the absence of drug). In addition to decreased vesicle formation, the X-irradiated cells also exhibited an altered drug distribution compared with cells exposed to DOX alone (see Fig. 4D). The DOX-treated cells displayed

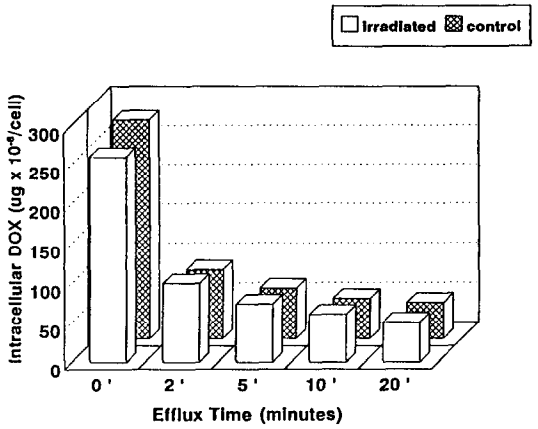

Fig. 9. Efflux of DOX determined using fluorescent spectrometry at 0, 2, 5, 10, and 20 min in 10 Gy irradiated or unirradiated control LZ-100 cells pre-exposed to 150 μg/mL DOX for 1 hr.

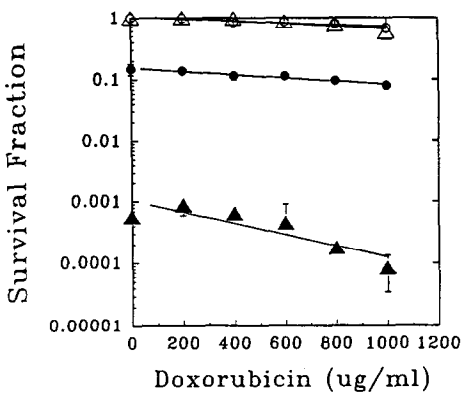

Fig. 10. Survival response of LZ-100 cells exposed to DOX for 1 hr (open circles) or pretreated with 5 Gy of X-rays before DOX exposure (closed circles). Cells exposed to DOX for 3 hr are represented by open triangles, while those pretreated with 10 Gy of X-rays are represented by closed triangles. Lines represent linear regression analysis of the points, which represent triplicate points from three independent experiments. The standard deviation is shown unless it was smaller than the symbol size.

an intracellular distribution like that previously described for panels A and B of Fig. 4. In contrast, the X-ray/DOX-treated cells contained fluorescence in both the nucleus and cytoplasm and had taken on an appearance more like that of wild-type V79 cells (compare panels C and D of Fig. 4). Thus, X-ray treatment at the time of DOX addition can decrease vesicle formation dramatically and also alter the drug distribution between nucleus and cytoplasm in LZ-100 cells.

If the inhibitory effect of radiation is a result of a biological response, it might be expected to exhibit a dose–response. To test this, LZ-100 cells were exposed to 0, 2, 5, 7.5, 10, or 20 Gy at the time of DOX (100 μg/mL) addition. Following a 2-hr incubation, the number of vesicles per cell was determined. The results, shown in Fig. 8, reveal that an increasing amount of inhibition of vesicles observed was seen with increasing radiation dose up to 10 Gy. From 10 to 20 Gy the inhibitory effect diminished.

To determine if the observed effects of radiation on intracellular DOX distribution and number of vesicles observed could be a result of inhibition of P-gp function in the cell membrane, DOX efflux was measured. Spectrophotometric analysis of DOX contained per cell was performed at 0, 2, 5, 10 and 20 min following a 1 hr exposure to 150 μg/mL DOX with/without pretreatment with 10 Gy of X-rays. The results in Fig. 9 show no difference between samples with or without irradiation. This suggests that irradiation does not affect P-gp efflux (within the limits of the detection method used) and that the effects observed are likely to be a consequence of damage to other cellular targets.

To test if vesicle formation might contribute to the enhanced DOX survival exhibited by LZ-100, cells were pretreated with either 5 or 10 Gy of X-rays to inhibit vesicle formation and then exposed to various concentrations of DOX for either 1 or 3 hr. As can be seen in Fig. 10, compared with cells receiving DOX treatment alone for 1 hr with a $K_i^{-1} = 2693$ (open circles), those receiving X-ray pretreatment exhibited decreased survival with a $K_i^{-1} = 1666$ (closed circles). A comparison of the survival fraction of cells treated with radiation alone and those receiving radiation and DOX treatment revealed an overall trend of decreasing survival with increasing concentrations of DOX. This effect became more evident in cells pretreated with 10 Gy of X-ray and exposed to the same concentrations of DOX for 3 hr [Fig. 10, compare samples receiving DOX only (open triangles) with a $K_i^{-1} = 1870$ with those receiving X-ray pretreatment before DOX (filled triangles) with a $K_i^{-1} = 517$]. These results suggest the possibility that sequestration of DOX in vesicles may be important for cell survival in LZ-100 cells.

Drug sequestration in vesicles has been reported previously in resistant cells following treatment with DOX, MITO [28], or DAUN. To determine if the drug sequestration phenomenon in LZ-100 is restricted to DOX or is present after treatment with other drugs, LZ-100 cells were exposed to 100 μg/mL MITO or DAUN and were examined for the presence of vesicles following a 2-hr treatment. Blue-colored vesicles, similar to those previously reported and characteristic of MITO [28], were observed in bright field or phase contrast viewing of LZ-100 cells, but fewer vesicles (average of 34.0 ± 8) were observed than with DOX (see Fig. 11). Red fluorescent vesicles, like those seen following DOX treatment, were present in cells treated with 100 μg/mL DAUN (data not shown), averaging 36.6 ± 6 vesicles per cell. Thus, drug-containing vesicles are seen following treatment with DAUN, MITO, or DOX, but significantly more vesicles were observed following DOX treatment.

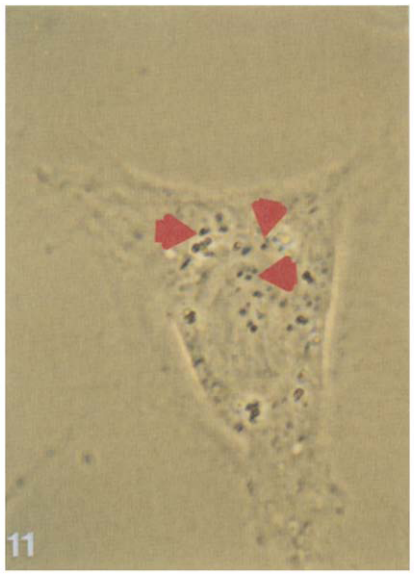

Fig. 11. LZ-100 cell treated with 100 μg/mL MITO for 2 hr and visualized with phase contrast microscopy. Arrows point to blue colored vesicles visible in this plane of focus. Additional vesicles are present throughout the cell in other focal planes.

DISCUSSION

These studies show that the increased drug resistance exhibited by LZ-100 cells compared with that by LZ-8 cells, is probably *not* related to levels of P-gp in the plasma membrane but may be related to the altered drug distribution of LZ-100 cells. Compared with wild-type V79 cells, LZ-100 cells exhibited decreased levels of DOX in the nucleus versus the cytoplasm, with DOX present in numerous cytoplasmic vesicles. The ability to form DOX-containing vesicles corresponded with the level of drug resistance exhibited by LZ cell lines but *not* with the level of P-gp in the plasma cell membrane. Exposure to radiation immediately prior to DOX treatment in LZ-100 cells dramatically decreased the number of vesicles observed (>½) and decreased cell survival without a detectable effect on P-gp-mediated drug efflux. Two other drugs, MITO and DAUN, were also observed to localize to cytoplasmic vesicles following exposure in LZ-100 cells.

Our previous studies have suggested that the high level of DOX resistance exhibited by LZ cell lines is a consequence of more than one mechanism [16–18]. As higher levels of resistance were achieved, the relative contribution of individual mechanisms toward the overall drug resistance appeared to change. Undoubtedly, enhanced drug efflux [16] resulting from the high levels of P-gp in the plasma membrane plays a significant role in all LZ cell lines. However, other resistance mechanisms must assume increased importance in LZ-100, since LZ-100 cells exhibit greater DOX resistance than LZ-8 cells in the light of equivalent levels of P-gp and drug efflux. This plateau in P-gp levels (observed at 20% of the total membrane proteins) in more highly resistant LZ cell lines may represent the physical limit of P-gp that a cell membrane can accommodate, a cellular requirement for less energy-requiring resistance mechanisms, or a down-regulation of the *pgp* 1 (hamster *mdr* 1) gene from feed-back control signals.

A second mechanism of resistance is a greatly enhanced ability to detoxify DOX in LZ-8 (and LZ-100) cells compared with wild-type V79 cells [18]. LZ cells structurally modify DOX to a cytotoxically inactive form which is extruded from the cell. Whether vesicles are involved in this process is currently under investigation. A third mechanism is a moderate reduction in topoisomerase II activity, compared with V79, for LZ-8 and LZ-100*. Although stabilized cleavable complex formation is reduced, the amount of decrease cannot, in and of itself, account for the high level of drug resistance observed in LZ cell lines. Enhanced DNA repair also does not appear to play a role in DOX resistance in LZ cells, but reduced initial DNA damage appears to have relevance [19]. Glutathione-*S*-transferase has been shown previously to be unaltered [29]. In addition to these previously described mechanisms, the studies reported here suggest the possibility that an altered drug distribution and drug sequestration may represent additional mechanisms contributing to drug resistance.

Different cell types have been shown to exhibit vesicles similar to those reported here in LZ-100 cells. Some of the types of cells in which drug-sequestering vesicles have been observed include: MITO- or DOX-resistant variants of HT29 [30], anthracycline- and alkaloid-resistant CEM/VLB human T-cell lymphomas [31], DOX-resistant MCF-7/ADR breast tumor cells [32], DAUN- or DOX-resistant P388 and Ehrlich ascites cells [33, 39], DOX-resistant rat colon cancer cells [20], various human gastric and colon carcinoma cell lines [28, 34], as well as primary human tumor cells [30]. Few or no drug-sequestering vesicles have been reported in wild-type or sensitive cells, consistent with our observations in V79 cells [28]. Thus, although the existence of vesicles in drug-resistant cells is well established, relatively little is known about their nature and function.

Vesicles have been postulated to play an important role in drug elimination [33, 35]. Some have suggested that vesicles may inactivate the sequestered drug prior to releasing it [28]. Drug may be extruded via exocytosis. Alternatively, if drug could escape from intracytoplasmic vesicles after inactivation, then inactivated drug may accumulate inside the cell [34]. Accumulated, inactivated drug could slow the entry of cytotoxically active drug from the exterior of the cell by establishing a concentration barrier. Also, any unaltered drug that passively diffuses into the cell could be pumped into pre-existing vesicles for inactivation if P-gp were present in the vesicle membrane, as some evidence suggests [30, 36].

Previous reports of drug-containing vesicles have suggested that they are formed either at the cell membrane via endocytosis or intracellularly in

* Unpublished observations.

the perinuclear area at/near the Golgi complex [13, 37, 38]. In cells selected for MITO resistance, vesicles appear to be formed from, and remain near, the plasma membrane until extrusion from the cell [28]. Due to a high rate of membrane turnover detected in some drug-resistant cells, a nonspecific- or nonreceptor-mediated endocytotic process has been proposed [33, 39]. However, if vesicles are formed via endocytosis in LZ-100 cells, it cannot be via a completely nonspecific process, since similar numbers of vesicles were not observed following similar exposure to DOX, MITO, and DAUN. Other reports have suggested that vesicles could be formed at/near the Golgi complex, a site of P-gp localization inside the cell [1, 12]. In this case, vesicles may be formed from drug removed from the nucleus or drug present in the cytoplasm [40]. However, in one study removal of drug from the nucleus has been shown to occur in the absence of vesicle formation [41]. In contrast with other reports, DOX does not appear to enter the nucleus to a significant extent (based on fluorescence) in LZ-100 cells; however, a large number of vesicles accumulate in the perinuclear area. In addition, vesicles are present throughout the cytoplasm and in the apical regions of many cells.

Our studies showed that radiation pretreatment dramatically inhibited DOX-induced vesicle formation in LZ-100 cells; this inhibition increased linearly with doses up to 10 Gy and resulted in a redistribution of DOX from mainly the cytoplasm to primarily the nucleus. This radiation effect does not appear to be related to repression of drug efflux via P-gp, since no alteration in efflux was detected in these studies between irradiated and unirradiated samples. The observations with LZ-100 described here might be explained by either damage to cellular membranes and/or damage registered at other radiation-sensitive sites (i.e. DNA) [25–27]. Membrane-induced damage from X-ray or DOX may contribute to cell death or lead to inhibition/retardation of DOX-containing vesicles formed at the plasma cell membrane via endocytosis. This might allow greater access of DOX to cellular target sites (i.e. DNA) and thereby influence cell killing. Radiation-induced damage either to the nuclear membrane or to the mechanism responsible for nuclear drug exclusion in LZ-100 cells might enable more DOX to enter the nucleus. This is consistent with the observations reported here in which DOX was present in the nucleus following irradiation. This redistribution of drug is similar to that reported following treatment of drug-resistant cells with verapamil and other MDR-reversing agents [37] and could result in the production of more DNA damage. Alternatively, the combined damage produced by radiation treatment at the time of DOX exposure might overwhelm DNA repair processes and cause decreased survival. However, this last alternative seems unlikely in view of our previous damage/repair studies with LZ-8, where no differences in either initial levels of DNA damage or types of DNA repair were detected [19, 42, 43].

Our results showed that exposure of LZ-100 cells to radiation decreased the number of DOX-containing vesicles formed by more than one-half and also decreased survival following DOX exposure. While these results suggest that vesicles may have some impact on cell survival, the effect on survival is not as dramatic as the inhibitory effect on vesicle formation. Since LZ-100 cells exhibit a "complex" MDR phenotype, multiple mechanisms contribute to the overall cell survival observed. Elucidating the contribution of one mechanism, when others also simultaneously contribute toward cell survival, is difficult. This may explain the lack of a noticeably larger response on cell survival in LZ-100. Future isolation of the gene(s) involved in drug sequestration and transfection into a drug-sensitive cell line would allow this question to be addressed unequivocally.

In these studies, DOX treatment was able to induce vesicle formation at nontoxic drug concentrations in LZ-3, LZ-8, and LZ-100 cells. This suggests that drug sequestration can occur in cells exhibiting different levels of drug resistance and that this phenomenon likely also occurs in cells exhibiting lower levels of drug resistance. This view is supported by other studies in which low level mitoxantrone (HT29NOV) and DOX (HT29ADR) resistant variants of HT29 cells exhibited vesicles following drug exposure [30]. In addition, vesicles have been observed in tumor preparations made from fresh human tumor biopsies. Those tumor preparations that exhibited vesicles were more resistant to DOX than were those without vesicles [30].

The concentrations of DOX utilized in these studies to visualize vesicles were high (1–100 μg/mL = 0.0018 to 0.18 mM), but noncytotoxic to the LZ cells. At high concentrations, DOX is known to self-associate and form dimers and/or n-mers [44, 45]. This association is temperature and pH dependent [46]. Under the treatment conditions used for LZ-100, such association is likely to have occurred. However, vesicles were observed in LZ-100 cells at concentrations in which no self-association is expected to occur (3 μg/mL). Thus, although it cannot be excluded that dimerization of DOX may play a role in vesicle formation, DOX self-association does not appear to be a requirement.

Some previous studies and our own unpublished observations suggest that P-gp is a component of the membranes of the cytoplasmic, drug-containing vesicles [36]. Although primarily invoked as an energy-dependent drug efflux pump [4], increasing evidence suggests that P-gp may also have additional functions [17, 18, 47, 48]. If DOX-containing vesicles form via endocytosis, the P-gp molecule would be expected to be oriented so that DOX could be pumped into the vesicle. Our data and that of others suggest the possibility that the P-gp molecule may serve as a binding site and play a role in vesicle formation [33, 39, 47]. In view of increasing evidence that MDR can be caused by a variety of mechanisms [1, 49] and the fact that current chemotherapeutic strategies may induce complex MDR [2] and drug sequestration in vesicles [30], it is essential to detail and identify the diverse mechanisms contributing to a complex MDR phenotype.

Acknowledgements—The expert assistance in computer graphics by Monique Tucker is gratefully acknowledged.

This research was supported by a grant from the National Cancer Institute, National Institutes of Health (CA 34269).

REFERENCES

1. Tiirikainen MI and Krusius T, Multidrug resistance. *Ann Med* **23**: 509–520, 1991.
2. Murren JR and Hait WN, Why haven't we cured multidrug resistant tumors? *Oncol Res* **4**: 1–6, 1992.
3. Bradley G, Juranka PF and Ling V, Mechanism of multidrug resistance. *Biochim Biophys Acta* **948**: 87–128, 1988.
4. Kane SE, Pastan I and Gottesman MM, Genetic basis of multidrug resistance of tumor cells. *J Bioenerg Biomembr* **22**: 593–618, 1990.
5. Weinstein RS, Kuszak JR, Kluskens LF and Coon JS, P-glycoproteins in pathology: The multidrug resistance gene family in humans. *Prog Pathol* **21**: 34–48, 1990.
6. Hammond JR, Johnstone RM and Gros P, Enhanced efflux of [^{3}H]vinblastine from Chinese hamster ovary cells transfected with a full-length complementary DNA clone for the *mdr*1 gene. *Cancer Res* **49**: 3867–3871, 1989.
7. Sinha BK, Katki AG, Batist G, Cowan KH and Myers CE, Differential formation of hydroxyl radicals by Adriamycin in sensitive and resistant MCF-7 human breast tumor cells: Implications for the mechanism of action. *Biochemistry* **26**: 3776–3781, 1987.
8. Fairchild CR and Cowan KH, Keynote address: Multidrug resistance: A pleiotropic response to cytotoxic drugs. *Int J Radiat Oncol Biol Phys* **20**: 361–367, 1991.
9. Morrow CS and Cowan KH, Glutathione *S*-transferases and drug resistance. *Cancer Cells* **2**: 15–22, 1990.
10. Beck WT, Mechanisms of multidrug resistance in human tumor cells. The roles of P-glycoprotein, DNA topoisomerase II, and other factors. *Cancer Treat Rev* **17**(Suppl A): 11–20, 1990.
11. Zijlstra JG, de Vries EGE and Mulder NH, Multifactorial drug resistance in an Adriamycin-resistant human small cell lung carcinoma cell line. *Cancer Res* **47**: 1780–1784, 1987.
12. Dietel M, What's new in cytostatic drug resistance and pathology. *Pathol Res Pract* **187**: 892–905, 1991.
13. Hindenburg AA, Gervasoni JE Jr, Krishna S, Stewart VJ, Rosado M, Lutzky J, Bhalla K, Baker MA and Taub RN, Intracellular distribution and pharmacokinetics of daunorubicin in anthracycline-sensitive and -resistant HL-60 cells. *Cancer Res* **49**: 4607–4614, 1989.
14. Weaver JL, Pine SP, Aszalos A, Schoenlein PV, Currier SJ, Padmanabhan R and Gottesman MM, Laser scanning and confocal microscopy of daunorubicin, doxorubicin, and rhodamine 123 in multidrug-resistant cells. *Exp Cell Res* **196**: 323–329, 1991.
15. Howell N, Belli TA, Zaczkiewicz LT and Belli JA, High-level, unstable Adriamycin resistance in a Chinese hamster mutant cell line with double minute chromosomes. *Cancer Res* **44**: 4023–4029, 1984.
16. Belli JA, Zhang Y and Fritz P, Transfer of Adriamycin resistance by fusion of M_r 170,000 P-glycoprotein to the plasma membrane of sensitive cells. *Cancer Res* **50**: 2191–2197, 1990.
17. Sognier MA, Zhang Y, Eberle RL and Belli JA, Characterization of Adriamycin-resistant and radiation-sensitive Chinese hamster cell lines. *Biochem Pharmacol* **44**: 1859–1868, 1992.
18. Zhang Y, Sweet KM, Sognier MA and Belli JA, An enhanced ability for transforming Adriamycin into a noncytotoxic form in a multidrug-resistant cell line (LZ-8). *Biochem Pharmacol* **44**: 1869–1877, 1992.
19. Sognier MA, Eberle RL, Zhang Y and Belli JA, Interaction between radiation and drug damage in mammalian cells. V. DNA damage and repair induced in LZ cells by Adriamycin and/or radiation. *Radiat Res* **126**: 80–87, 1991.
20. Chauffert B, Martin F, Caignard A, Jeannin J-F and Leclerc A, Cytofluorescence localization of Adriamycin in resistant colon cancer cells. *Cancer Chemother Pharmacol* **13**: 4–18, 1984.
21. Altenberg GA, Stoddard JS and Reuss L, Electrophysiological effects of basolateral [Na^+] in *Necturus* gallbladder epithelium. *J Gen Physiol* **99**: 241–262, 1992.
22. Sognier MA, Neft RE, Roe AL, Eberle RL and Belli JA, Dot-blot hybridization: Quantitative analysis with direct beta counting. *Biotechniques* **11**: 520–525, 1991.
23. Tapiero H, Munck J-N, Fourcade A and Lampidis TJ, Cross-resistance to rhodamine 123 in Adriamycin- and daunorubicin-resistant Friend leukemia cell variants. *Cancer Res* **44**: 5544–5549, 1984.
24. Lee J-S, Paull K, Monks A, Hose C, Alvarez M, Grever M, Fojo A and Bates S, Rhodamine 123 efflux in the 60 cell lines of the NCI's new drug screen: Sensitivity, correlation with *mdr*-1 expression, and value in identifying P-glycoprotein substrates. *Proc Am Assoc Cancer Res* **34**: 317, 1993.
25. Ward JF, DNA damage produced by ionizing radiation in mammalian cells: Identities, mechanisms of formation, and repairability. *Prog Nucleic Acid Res Mol Biol* **35**: 95–125, 1988.
26. Raleigh RJ, Radioprotection of membranes. *Pharmacol Ther* **39**: 109–113, 1988.
27. Somosy Z, Csuka O, Kubasova T, Kovacs J and Koteles GJ, Surface heterogeneity of tumor cells and changes upon ionizing radiation. *Scanning Microsc* **3**: 895–906, 1989.
28. Dietel M, Arps H, Lage H and Niendorf A, Membrane vesicle formation due to acquired mitoxantrone resistance in human gastric carcinoma cell line EPG85-257. *Cancer Res* **50**: 6100–6106, 1990.
29. Medh RD, Gupta V, Zhang Y, Awasthi YC and Belli JA, Glutathione *S*-transferase and P-glycoprotein in multidrug resistant Chinese hamster cells. *Biochem Pharmacol* **39**: 1641–1645, 1990.
30. Seidel A, Kaufmann O and Dietel M, Intracellular distribution of cytostatic drugs in low degree resistant tumor cell lines and primary tumor cell preparations. *Proc Am Assoc Cancer Res* **34**: 25, 1993.
31. Zamora JM and Beck WT, Chloroquine enhancement of anticancer drug cytotoxicity in multiple drug resistant human leukemic cells. *Biochem Pharmacol* **35**: 4303–4310, 1986.
32. Gervasoni JE Jr, Fields SZ, Krishna S, Baker MA, Rosado M, Thuraisamy K, Hindenburg AA and Taub RN, Subcellular distribution of daunorubicin in P-glycoprotein-positive and -negative drug-resistant cell lines using laser-assisted confocal microscopy. *Cancer Res* **51**: 4955–4963, 1992.
33. Sehested M, Skovsgaard T, van Deurs B and Winther-Nielsen H, Increase in nonspecific adsorptive endocytosis in anthracycline- and vinca alkaloid-resistant Ehrlich ascites tumor cell lines. *J Natl Cancer Inst* **78**: 171–177, 1987.
34. Boiocchi M and Toffoli G, Mechanism of multidrug resistance in human tumour cell lines and complete reversion of cellular resistance. *Eur J Cancer* **28A**: 1099–1105, 1992.
35. Beck WT, The cell biology of multiple drug resistance. *Biochem Pharmacol* **36**: 2879–2887, 1987.
36. Dietel M and Arps A, Immunocytochemical evidence of P 170 positive, mitoxantrone (DHAD) containing vesicles and structurally altered microtubules in a human gastric carcinoma cell line with atypical multidrug resistance (mdr). *Proc Am Assoc Cancer Res* **30**: 178, 1989.

37. Schuurhuis GJ, Broxterman HJ, Cervantes A, van Heijningen THM, de Lange JHM, Baak JPA, Pinedo HM and Lankelma J, Quantitative determination factors contributing to doxorubicin resistance in multidrug-resistant cells. *J Natl Cancer Inst* **81**: 1887–1992, 1989.
38. Klohs WD and Steinkampf RW, The effect of lysosomotropic agents and secretory inhibitors on anthracycline retention and activity in multiple drug-resistant cells. *Mol Pharmacol* **34**: 180–185, 1988.
39. Sehested M, Skovsgaard T, van Deurs B and Winther-Nielsen H, Increased plasma membrane traffic in daunorubicin resistant P388 leukaemic cells. Effect of daunorubicin and verapamil. *Br J Cancer* **56**: 747–751, 1987.
40. Dietel M, Seidel A and Nickelsen M, Microfilaments and vesicle associated drug transport in multidrug resistant EPG85-257 cells. *Proc Am Assoc Cancer Res* **33**: 430, 1992.
41. Marquardt D and Center MS, Drug transport mechanisms in HL60 cells isolated for resistance to Adriamycin: Evidence for nuclear drug accumulation and redistribution in resistant cells. *Cancer Res* **52**: 3157–3163, 1992.
42. Belli JA, Interaction between radiation and drug damage in mammalian cells. IV. Radiation response of Adriamycin-resistant V79 cells. *Radiat Res* **119**: 88–100, 1989.
43. Zhang Y, Sweet KM, Sognier MA and Belli JA, Interaction between radiation and drug damage in mammalian cells. VI. Radiation and doxorubicin age-response function of doxorubicin-sensitive and -resistant Chinese hamster cells. *Radiat Res* **132**: 105–111, 1992.
44. Barthelemy-Clavey V, Maurizot J-C, Dimicoli J-L and Sicard P, Self-association of daunorubicin. *FEBS Lett* **46**: 5–10, 1974.
45. Chaires JB, Dattagupta N and Crothers DM, Self-association of daunomycin. *Biochemistry* **21**: 3927–3932, 1982.
46. Rivory LP, Pond S and Winzor DJ, The influence of pH on the interaction of lipophilic anthracyclines with bovine serum albumin. *Biochem Pharmacol* **44**: 2347–2355, 1992.
47. Warren L, Jardillier JC and Ordentlich P, Secretion of lysosomal enzymes by drug-sensitive and multiple drug-resistant cells. *Cancer Res* **51**: 1996–2001, 1991.
48. Gill DR, Hyde SC, Higgins CF, Valverde MA, Mintenig GM and Sepúlveda FV, Separation of drug transport and chloride channel functions of the human multidrug resistance P-glycoprotein. *Cell* **71**: 23–32, 1992.
49. Harris AL and Hochhauser D, Mechanisms of multidrug resistance in cancer treatment. *Acta Oncol* **31**: 205–213, 1992.